

# Band gap of essentially fourfold-coordinated amorphous diamond synthesized from C<sub>60</sub> fullerene

H. Hirai

*Institute of Geoscience, University of Tsukuba, Tsukuba, Ibaraki 305-8571, Japan*

M. Terauchi and M. Tanaka

*Research Institute for Scientific and Measurements, Tohoku University, Aoba-ku, Sendai 980-8577, Japan*

K. Kondo

*Materials and Structures Laboratory, Tokyo Institute of Technology, Nagatsuta, Yokohama 226, Japan*

(Received 3 December 1998; revised manuscript received 5 April 1999)

The band gap and density of state for a form of amorphous diamond synthesized from C<sub>60</sub> fullerene by shock compression were measured by electron energy-loss spectroscopy in this study. The dielectric functions of the material were derived from the loss function obtained from its spectrum by Kramers-Kronig transformation. The imaginary part of the dielectric function,  $\epsilon_2$ , showed that the magnitude of the gap was up to 4.5 eV, somewhat smaller than that of crystalline diamond, which is 5.5 eV, but larger than those of any other amorphous material reported before. The excitation of interband transition was observed only at the  $\Gamma$  point, not at the  $X$  and  $L$  points. The density of state around the gap was rather broad. The radial distribution function analysis made previously revealed that the carbon atoms of the material were tetrahedrally coordinated; furthermore, these tetrahedra were arranged in the same manner as that of crystalline diamond within the region of unit cell size. The characteristic electronic properties of the amorphous diamond measured were consistently attributable to the unique atomic configuration of the material. The band gap and density of state were discussed in relation to the fraction of fourfold coordination, the density, and the short-range structure, comparing with other amorphous carbon materials. [S0163-1829(99)14033-5]

## INTRODUCTION

Various bonding states of carbon allow it to form a wide variety of phases involving crystalline and noncrystalline forms. In the noncrystalline forms, especially not only pure twofold coordination, threefold coordination, and fourfold coordination, but also their modified coordination (deformed from pure coordination) or combined coordination (i.e., more than two coordinations are included in a material) may exist more easily because there is less constraint from a long-range order structure. The relationship between the topology of coordination and the physical properties derived from it is currently a hot issue, as researchers attempt to understand such fundamental physics as the evolution of the bonding state of carbon and its technological applications. Intensive studies have been directed toward the preparation by various deposition technique such as mass selected ion beam deposition<sup>1-7</sup> and filtered cathodic vacuum arc deposition,<sup>8-16</sup> pulsed laser arc deposition,<sup>17</sup> and plasma assisted chemical vapor deposition (CVD),<sup>18</sup> as well as towards the characterization of the materials by various spectroscopy and diffractometry such as electron energy-loss spectroscopy (EELS),<sup>5,9,11,17,18</sup> Raman,<sup>1,19,20,21</sup> other spectroscopy,<sup>2,4,5,10,22,23</sup> and radial distribution function (RDF) analysis.<sup>1,8,14,15,24</sup> In addition, theoretical calculations on structures and properties were carried out.<sup>25,26</sup> One of the goals is to synthesize highly tetrahedrally coordinated amorphous carbon (ta-C) of which properties are comparable to those of crystalline diamond; thus several ta-C materials having more than 80% fourfold coordination were obtained so far, for instance, 92% ta-C material,<sup>14</sup> 87% ta-C,<sup>9</sup> 85% ta-C,<sup>2</sup>

and 83% ta-C.<sup>8</sup> And, their electronic and/or optical properties<sup>1,3,4,11,17,22,25,26</sup> such as band gap and resistivity, mechanical properties<sup>1,5,10</sup> such as hardness, bulk modulus, and internal stress, and also thermal properties<sup>23</sup> were also examined.

Among those studies, a form of transparent amorphous diamond, consisting of mostly fourfold coordination, was successfully fabricated by the present authors.<sup>27</sup> They made effective use of the potential of C<sub>60</sub> fullerene to transform to diamond<sup>28</sup> and also of the advantage of the shock-compression and rapid-quenching technique, which involves pulse loading of high pressure and high temperature with subsequent rapid quenching.<sup>29</sup> X-ray and electron diffractometry revealed that the material was amorphous in long-range order, and EELS showed it to be diamond in short-range order.<sup>27</sup> The transition process—that is, changes in electronic state and structure from C<sub>60</sub> fullerene to amorphous diamond under shock compression—as examined by EELS and electron diffractometry,<sup>30</sup> was uniquely different from those of graphite-based materials. In addition, the structure in short-range order was confirmed by RDF analysis to demonstrate the characteristic configuration of carbon atoms.<sup>31</sup> The tetrahedra of carbon atoms were arranged in the same manner as those of crystalline diamond within a region of unit-cell size. This short-range structure was distinguishable from those of ta-C materials reported before. Therefore, electronic and optical properties such as the magnitude of gap and the density of state (DOS) around the gap are of great interest for clarifying the hidden nature of the material and for developing practical uses. Band gap usually is measured by a conventional optical absorption method<sup>1,3</sup> and

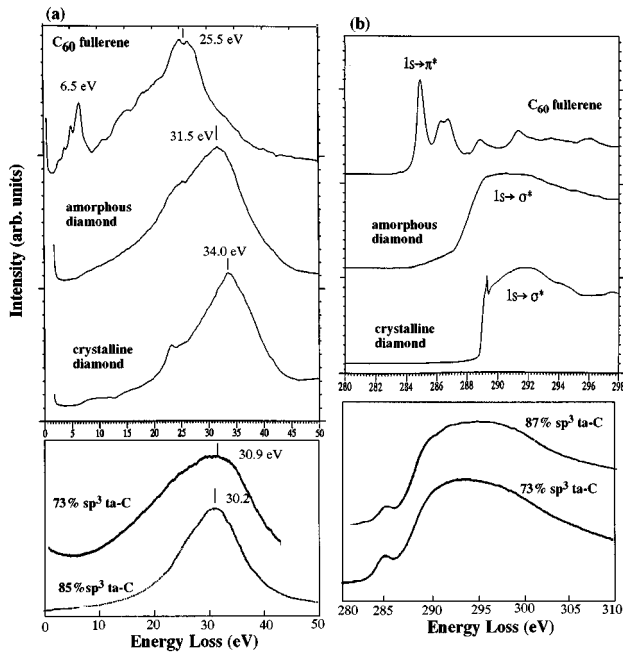


FIG. 1. High-resolution EELS spectra of (a) plasmon region and (b) inner shell excitation region,  $k$ -edge of carbon, for  $C_{60}$  fullerene, the present amorphous diamond, and crystalline diamond. For comparison, plasmon spectra for 73%  $sp^3$  ta-C [Merkulov *et al.* (Ref. 17)] and for 85%  $sp^3$  [Berger, McKenzie, and Martin (Ref. 16)], and  $k$ -edge spectra for 87%  $sp^3$  ta-C [Ravi *et al.* (Ref. 9)] and 73%  $sp^3$  ta-C [Merkulov *et al.* (Ref. 17)] are shown (each bottom). A sharp peak observed in the  $k$ -edge spectrum for the crystalline diamond is assigned to exciton.

spectroscopic ellipsometry,<sup>4,7,17</sup> but the present amorphous diamond was too small (a few tens of a micrometer to 100 micrometers) and irregularly shaped<sup>27</sup> to be measured by the conventional optical method. Thus, this study adopted a technique estimating band gap from EELS spectrum. The estimated band gap was discussed in relation to the fraction of fourfold coordination ( $sp^3$  bonding), density and RDF, comparing with other ta-C materials reported before.

## EXPERIMENT

An optical absorption method can directly obtain the imaginary part of the dielectric function,  $\epsilon_2$ , associated with a single electron excitation of interband transition. Electron energy-loss spectroscopy does not directly give  $\epsilon_2$ , but an EELS spectrum is related to the dielectric function by simple equation,<sup>32</sup> so that the real and the imaginary parts of the dielectric function,  $\epsilon_1$  and  $\epsilon_2$ , can be obtained by Kramers-Kronig analysis of the loss function ( $\text{Im}[-1/\epsilon]$ ) obtained from the EELS spectrum. For such analysis, a high-energy-resolution EELS spectrum is indispensable, and so the present measurements were made using a special high-energy-resolution electron energy loss spectrometer based on a transmission electron microscope.<sup>33</sup> The energy-resolution of the present measurement was 0.2 eV. The analytical procedure used in the present study was the same as those described previously.<sup>33,34</sup> To confirm the reliability of the present method, natural crystalline diamond was also examined. The inner shell excitation, near  $K$ -edge of carbon,

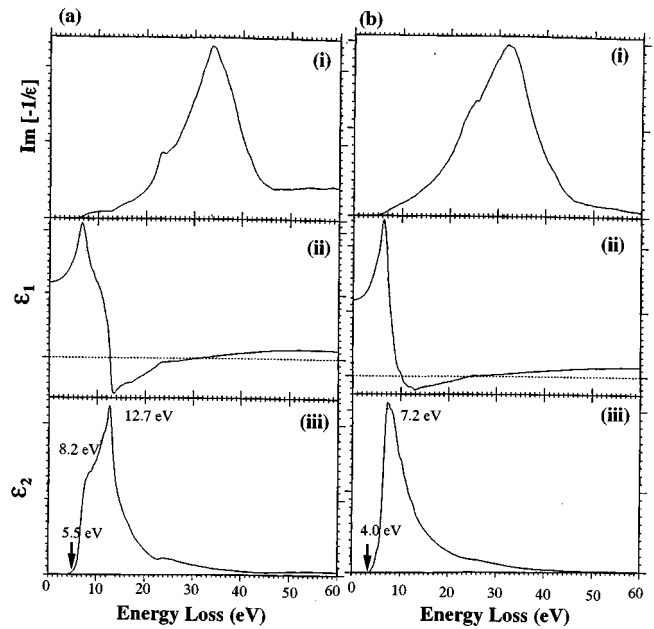


FIG. 2. Loss function (i), the real part (ii), and imaginary part (iii) of the dielectric function for natural crystalline diamond (a) and for amorphous diamond (b). For the amorphous diamond, the magnitude of 4.0 eV is approximately the middle value among the sample fragments measured.

which reflects the distribution of the density of state in the conduction bands, was also measured by the high-energy-resolution EELS apparatus with the energy resolution of 0.2 eV.

## RESULTS

Representative high-resolution EELS spectra for  $C_{60}$  fullerene, amorphous diamond, and natural crystalline diamond in the plasmon region (0 to 50 eV) and in the inner shell excitation region (280 to 298 eV) are shown in Fig. 1(a) (top) and Fig. 1(b) (top), respectively. For the  $C_{60}$  fullerene, the peak around 6.5 eV and peak around 285 eV were attributed to  $\pi \rightarrow \pi^*$  transition<sup>33</sup> and  $1s \rightarrow \pi^*$  transition, respectively. These peaks were completely absent for the amorphous diamond. For other highly fourfold-coordinated materials, 87%  $sp^3$  ta-C (Ref. 9) and 73%  $sp^3$ , ta-C,<sup>17</sup> the  $1s \rightarrow \pi^*$  transition peak was clearly observed [Fig. 1(b) (bottom)]. These results indicate that the amorphous diamond does not possess  $\pi$  electrons. The  $\sigma$ -plasmon, volume plasmon, peak for the amorphous diamond was 31.5 eV, while those of 85%  $sp^3$  ta-C material and 73%  $sp^3$  ta-C material are 30.2 (Ref. 16) and 30.9 eV,<sup>17</sup> respectively [Fig. 1(a) (bottom)]. In the inner shell excitation spectrum, the rising up of  $1s \rightarrow \sigma^*$  of amorphous diamond was rather gradual than that of the crystalline diamond, suggesting broadening of the DOS around the gap.

Figure 2 shows the loss function ( $\text{Im}[-1/\epsilon]$ ), the real part ( $\epsilon_1$ ), and the imaginary part ( $\epsilon_2$ ) of the dielectric function calculated from Fig. 1(a) for the crystalline diamond [Fig. 2(a)] and for the amorphous diamond [Fig. 2(b)]. The loss function was obtained by removing contributions from multiple scattering using the Fourier-log deconvolution

method and by using the refractive index,  $n = 2.42$ , of crystalline diamond. The dielectric function was derived from the loss function using Kramers-Kronig analysis. For the crystalline diamond, the onset energy of the spectrum (the band gap energy) was 5.5 eV [Fig. 2(a)(iii)], in excellent agreement with the established band gap of diamond (5.5 eV). Two peaks appeared at 8.2 and 12.7 eV in the  $\epsilon_2$  and were assigned to interband transitions at the  $\Gamma$  point and at  $X$  and  $L$  points, respectively.<sup>35,36</sup> For the amorphous diamond, the intensity increase at the onset was broader than that of the crystalline diamond [Fig. 2(b)(iii)], indicating a broader DOS. The onset energy varied from 3.5 to 4.5 eV with the sample fragments. A prominent peak was observed at 7.2 eV, which may correspond to the  $\Gamma$ -point transition [Fig. 2(b)(iii)]. Very little of the structure corresponding to the  $X$  and  $L$  points transition was seen.

## DISCUSSION

The  $\epsilon_2$  of the natural crystalline diamond, determined from the EELS spectrum, exhibited almost the same onset energy (band gap energy) and peak energy of  $\Gamma$ ,  $X$ , and  $L$  points as that obtained by optical measurement.<sup>36</sup> This result indicates that the technique estimating  $\epsilon_2$  from EELS spectra was sufficiently reliable. Summarizing the results for the amorphous diamond, the  $\epsilon_2$  obtained showed the band gap of up to 4.5 eV, and the DOS around the gap was somewhat broader than in natural diamond. In addition, the excitation occurred only at the  $\Gamma$  point, and the excitations at the  $X$  and  $L$  points were either not detected or considerably weakened. These characteristics are probably originated from the fraction of  $sp^3$  bonding, the density and the short-range structure as discussed below.

### A. Magnitude of band gap, $sp^3$ fraction, and density

Figure 3(a) shows optical (band) gaps of amorphous carbon materials reported before. The magnitude of the band gap of the present material was 3.5 to 4.5 eV. The variation of the magnitude was probably due to the synthetic condition, mainly shock temperature. In any case, the band gap measured was larger than any other ta-C material reported before [Fig. 3(a)].<sup>1,4,8,17</sup> Conductivity or resistivity of amorphous carbon is controlled mainly by fraction of  $sp^2$  bonding or that of  $sp^3$  bonding,<sup>3,10,17,25</sup> thus the large band gap of the amorphous diamond suggests extremely high fraction of  $sp^3$  bonding. Fraction of  $sp^3$  bonding is usually estimated by plasmon peak energy.<sup>37,10,11,1</sup> The plasmon peak energy of the present material, 31.5 eV, is the highest among the ta-C materials mentioned above. According to the relationship between  $sp^3$  fraction and plasmon peak energy,<sup>10,17,37</sup> the present material can be regarded as a mostly 100%  $sp^3$ -bonded material.

Fraction of  $sp^3$  bonding is also related to density of carbon materials.<sup>1,9,11,13</sup> Figure 3(b) represents variation of density in terms of  $sp^3$  fraction. The high fraction of  $sp^3$  bonding estimated for the present amorphous diamond suggests quite high density. Actually, the density of the material measured by a floating method was higher than 3.3 g/cm<sup>3</sup>, because the material completely sank down into diiodomethane (CH<sub>2</sub>I<sub>2</sub>; density: 3.3 g/cm<sup>3</sup>). No denser liquid

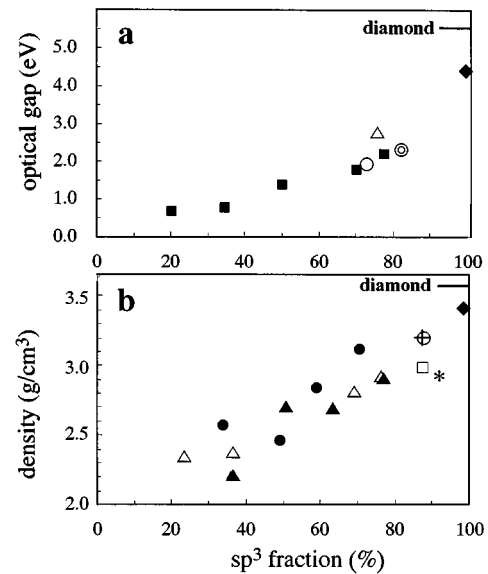


FIG. 3. (a) Variation of optical (band) gap versus to  $sp^3$  fraction for amorphous carbon materials. Solid rhombus: the present amorphous diamond; open circle: Merkulov *et al.* (Ref. 17); solid square: Lee *et al.* (Ref. 4); double circles: Chhowalla *et al.* (Ref. 8); open triangle: Weiler *et al.* (Ref. 1). (b) The variation of density versus  $sp^3$  fraction for ta-C materials. Solid rhombus: the present amorphous diamond; cross-hatched circle: Ravi *et al.* (Ref. 9); open square: Pharr *et al.* (Ref. 10); open triangle: Weiler *et al.* (Ref. 1); solid circle: McKenzie *et al.* (Ref. 13); solid triangle: Fallon *et al.* (Ref. 11); asterisk: McKenzie, Muller, and Pailthorpe (Ref. 14).

for measuring density was available because of safety for health. Considering the plasmon peak energies, which depend on electron density, of the present amorphous diamond and the crystalline diamond, 31.5 and 34.0 eV, respectively, the density of the amorphous diamond is less than that of crystalline diamond (3.51 g/cm<sup>3</sup>). The true density, thus, may be in the range from 3.3 to 3.5 g/cm<sup>3</sup>. The value of 3.3 g/cm<sup>3</sup>, in spite of the smallest estimation, is the higher than those of other ta-C materials reported [Fig. 3(b)].<sup>1,9-11,13,14</sup> The largest band gap of the present material, up to 4.5 eV, might be ascribed to its mostly 100%  $sp^3$  fraction and to its density higher than 3.3 g/cm<sup>3</sup>. The high density and high  $sp^3$  fraction are confirmed by the short-range structure by RDF analysis.

### B. Short-range structure by RDF analysis

RDF gives a most probable information of short-range structure, such as distance between atoms and the number of coordination, so the RDF analysis were made for the amorphous diamond.<sup>31</sup> Figure 4 shows comparison of the RDF with other highly tetrahedrally coordinated materials, one is 83%  $sp^3$  ta-C,<sup>8</sup> other is 92%  $sp^3$  ta-C.<sup>14</sup> The RDF obtained for the present amorphous diamond was evidently characterized by the third peak at 0.312 nm. This peak was not observed for those amorphous materials. The third distance corresponds to the distance from the center atom of a tetrahedron to the apexes of the neighboring tetrahedra. This topology means that the carbon atoms were, of course, tetrahedrally coordinated, and each apex atom of the tetrahedron

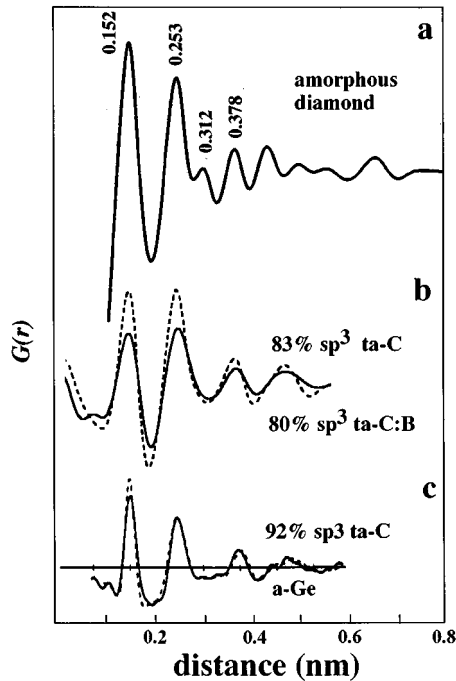


FIG. 4. Radial distribution function of highly ta-C materials. (a) The present amorphous diamond. (b) Solid line: 83%  $sp^3$  ta-C; broken line: 80%  $sp^3$  ta-C:B containing 4% B [Chhowalla *et al.*, (Ref. 8)]. (c) Solid line: 92%  $sp^3$  ta-C; broken line: a-Ge with reduced cell [McKenzie, Muller, and Pailthorpe (Ref. 14)]. The present amorphous diamond is distinguished by the third peak centered at 0.312 nm from other ta-C materials.

was furthermore surrounded by another tetrahedron. The tetrahedra thus were arranged in the same manner as those of crystalline diamond, within a region corresponding to the unit-cell size of crystalline diamond; in other words, this material consisted of randomly arranged unit-cell-sized diamond. The present amorphous diamond therefore can be evidently distinguished from other amorphous materials consisting only of randomly distributed tetrahedral clusters.

The  $\epsilon_2$  obtained for the present amorphous diamond indicated that excitation occurred only at the  $\Gamma$  point; excitations at the  $X$  and  $L$  points were either not detected or considerably weakened. This unique phenomenon can be reasonably explained by the short-range structure above mentioned.  $\Gamma$  point is independent of direction and periodicity of material because the wave number vector is zero, whereas  $X$  and  $L$  points are defined by a certain direction and periodicity of the material because the wave number vectors have defined values. In the case of the present amorphous diamond, only excitation independent of direction and periodicity of diamond occurred, but excitations dependent on direction and periodicity of diamond did not occur. Because the present material is regarded as to consist of randomly arranged unit-cell-sized diamond, only phenomenon independent of periodicity and direction could arise, but phenomenon dependent on them could not arise.

### C. Density of state

Theoretical analyses of DOS were made for several DLC materials to understand electronic and optical properties.<sup>25,26</sup>

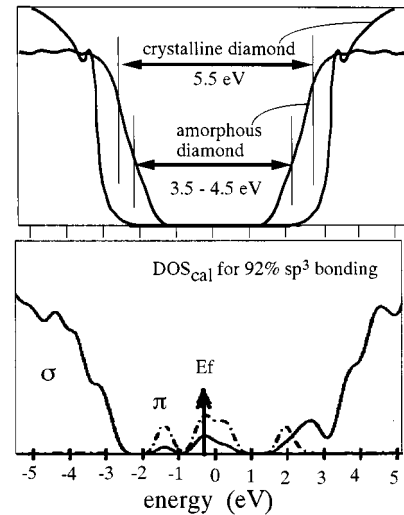


FIG. 5. Schematic illustration of hypothetical DOS for the present amorphous diamond and for the crystalline diamond drawn from the inner shell excitation spectra (top). A theoretically calculated DOS for 92%  $sp^3$ -bonded material by Robertson (Ref. 25) is shown for comparison (bottom).

Inner shell excitation spectrum and  $\epsilon_2$  reflect distribution of DOS, then rough information of the DOS can be obtained from these spectra. For the present material, the onset of the  $\epsilon_2$  was gradual [Fig. 2(b)(iii)], as well as that of the inner shell excitation spectrum was gradual [Fig. 1(b)]. These results suggest the DOS at the band edge of the conduction and/or valence band is broad. Assuming the inner shell spectrum measured as the distribution of electrons, hypothetical DOS was drawn for the present material and crystalline diamond (Fig. 5). The hypothetical DOS of the amorphous diamond exhibits broader and narrower gap (3.5 to 4.5 eV) than the DOS of the crystalline diamond dose sharper and wider gap (5.5 eV). Comparing the former DOS with the DOS theoretically calculated for 92%  $sp^3$  ta-C,<sup>25</sup> the former is more defined and wider gap. It is known that broadening of DOS is caused by disordering of atomic configuration, thus the broadening of DOS observed in the material might be brought about by the lack of periodicity in long-range order.

### D. Essentially fourfold-coordinated amorphous diamond

On the basis of the characterizations on band gap, fraction of  $sp^3$  bonding, density, short-range structure, the present amorphous diamond can be evaluated as essentially fourfold-coordinated amorphous diamond closest to crystalline diamond. The main reasons why such amorphous material was produced are considered to be (1) the bonding nature of  $C_{60}$  fullerene as the initial material and (2) its compression process;  $C_{60}$  fullerene possesses highly modified threefold coordination, nearer to fourfold coordination, because the bond angle,  $108^\circ$ , in the five-member rings is comparable to the bond angle of  $109.47^\circ$  in an ideal fourfold coordination. On the way of compression,  $C_{60}$  fullerene is polymerized before collapsing of  $C_{60}$  molecule.<sup>38,39</sup> When polymerization takes place, the carbon atoms bridging  $C_{60}$  molecules form fourfold coordination.<sup>39</sup> Such fourfold-coordinated carbon atoms are homogeneously distributed by every subnanometer



throughout the polymerized structure already. By further compression  $C_{60}$  molecules are relatively easily reproduced as an amorphous material consisting mostly of fourfold coordination which is more favorable under high pressure. Variation in the magnitude of the band gap for the amorphous diamond may be attributable to different degrees in

the ordering of atoms, which was mainly dependent on the temperature distribution in the sample capsule during shock synthesis.<sup>30</sup> Finally, the present technique estimating dielectric function from EELS spectrum was proved to be highly reliable and also quite useful for characterizing the electronic properties of small materials or small amount of materials.

- <sup>1</sup>M. Weiler, S. Sattel, T. Giessen, K. Jung, H. Ehrhardt, V. S. Veerasamy, and J. Robertson, *Phys. Rev. B* **53**, 1594 (1996).
- <sup>2</sup>C. Ronning, E. Dreher, J.-U. Thiele, P. Oelhafen, and H. Hofsass, *Diamond Relat. Mater.* **6**, 830 (1997).
- <sup>3</sup>A. Wei, D. Chen, S. Peng, N. Ke, and S. P. Wong, *Diamond Relat. Mater.* **6**, 983 (1997).
- <sup>4</sup>J. Lee, R. W. Collins, V. S. Veerasamy, and J. Robertson, *Diamond Relat. Mater.* **7**, 999 (1998).
- <sup>5</sup>Y. Lifshitz, G. D. Lempert, E. Grossman, I. Avigal, C. Uzan-Saguy, R. Kalish, J. Kulik, D. Marton, and J. W. Rabalais, *Diamond Relat. Mater.* **4**, 318 (1995).
- <sup>6</sup>M. Weiler, S. Sattel, K. Jung, H. Ehrhardt, V. S. Veerasamy, and J. Robertson, *Appl. Phys. Lett.* **64**, 2797 (1994).
- <sup>7</sup>J. Lee, R. W. Collins, V. S. Veerasamy, and J. Robertson, *J. Non-Cryst. Solids* **227-230**, 617 (1998).
- <sup>8</sup>M. Chhowalla, Y. Yin, G. A. J. Amaratunga, D. R. McKenzie, and T. Frauenheim, *Diamond Relat. Mater.* **6**, 207 (1997).
- <sup>9</sup>S. Ravi, P. Silva, Shi Xu, X. Tay, H. S. Tan, and W. I. Milne, *Appl. Phys. Lett.* **69**, 491 (1996).
- <sup>10</sup>G. M. Pharr, D. L. Callahan, S. D. Mcadams, T. Y. Tsui, S. Anders, A. Anders, J. W. Ager, I. G. Brown, C. S. Bhatia, S. R. P. Silva, and J. Robertson, *Appl. Phys. Lett.* **68**, 779 (1996).
- <sup>11</sup>P. J. Fallon, V. S. Veerasamy, C. A. Davis, J. Robertson, G. A. J. Amaratunga, and W. I. Milne, *Phys. Rev. B* **48**, 4777 (1993).
- <sup>12</sup>S. R. P. Silva, Shi Xu, B. K. Tay, H. S. Tan, H.-J. Scheibe, M. Chhowalla, and W. I. Milne, *Thin Solid Films* **291**, 317 (1997).
- <sup>13</sup>D. R. McKenzie, D. Muller, B. A. Pailthorpe, Z. H. Wang, E. Kravtchinskaiia, D. Segal, P. B. Lukins, P. D. Swift, P. J. Martin, G. Amaratunga, P. H. Gaskell, and A. Saeed, *Diamond Relat. Mater.* **1**, 51 (1991).
- <sup>14</sup>D. R. McKenzie, D. Muller, and B. A. Pailthorpe, *Phys. Rev. Lett.* **67**, 773 (1991).
- <sup>15</sup>F. Li and J. S. Lannin, *Phys. Rev. Lett.* **65**, 1905 (1990).
- <sup>16</sup>S. D. Berger, D. R. McKenzie, and P. J. Martin, *Philos. Mag. Lett.* **57**, 285 (1988).
- <sup>17</sup>V. I. Merkulov, D. H. Lowndes, G. E. Jellison, A. A. Puretzky, and D. B. Geohegan, *Appl. Phys. Lett.* **73**, 2591 (1998).
- <sup>18</sup>L. Ponsoonnet, C. Donnet, K. Varlot, J. M. Martin, A. Grill, and V. Patel, *Thin Solid Films* **319**, 97 (1998).
- <sup>19</sup>E. Rzepka, A. Lusson, E. A. Ponomarev, K. Mukhopadhyay, M. Sharon, and C. Levyclement, *Carbon* **36**, 587 (1998).
- <sup>20</sup>K. W. R. Gilkes, H. S. Sands, D. N. Batchelder, W. I. Milne, and J. Robertson, *J. Non-Cryst. Solids* **227-230**, 612 (1998).
- <sup>21</sup>S. Prawer, K. W. Nugent, and D. N. Jamieson, *Diamond Relat. Mater.* **7**, 106 (1998).
- <sup>22</sup>D. P. Dowling, K. Donnelly, M. Monclus, and M. McGuinness, *Diamond Relat. Mater.* **7**, 432 (1998).
- <sup>23</sup>C. J. Morath, H. J. Maris, J. J. Cuomo, D. L. Pappas, A. Grill, V. V. Patel, J. P. Doyle, and K. L. Saenger, *J. Appl. Phys.* **76**, 2636 (1994).
- <sup>24</sup>D. J. H. Cockayne and D. R. McKenzie, *Acta Crystallogr., Sect. A: Found. Crystallogr.* **A44**, 870 (1988).
- <sup>25</sup>J. Robertson, *Diamond Relat. Mater.* **6**, 212 (1997).
- <sup>26</sup>G. Jungnickel, Th. Kohler, Th. Frauenheim, M. Haase, P. Blau-deck, and U. Stephan, *Diamond Relat. Mater.* **5**, 175 (1996).
- <sup>27</sup>H. Hirai, K. Kondo, N. Yoshizawa, and Me. Shiraiishi, *Appl. Phys. Lett.* **64**, 1797 (1994).
- <sup>28</sup>H. Hirai, K. Kondo, and T. Oowada, *Carbon* **31**, 1095 (1993).
- <sup>29</sup>H. Hirai and K. Kondo, *Science* **253**, 772 (1991).
- <sup>30</sup>H. Hirai and K. Kondo, *Phys. Rev. B* **51**, 15555 (1995).
- <sup>31</sup>H. Hirai, Y. Tabira, K. Kondo, T. Oikawa, and N. Ishizawa, *Phys. Rev. B* **52**, 6162 (1995).
- <sup>32</sup>R. F. Egerton, *Electron Energy Loss Spectroscopy in the Electron Microscope* (Plenum, New York, 1966), p. 152.
- <sup>33</sup>R. Kuzuo, M. Terauchi, M. Tanaka, Y. Saito, and H. Shinohara, *Jpn. J. Appl. Phys., Part 1* **30**, 1817 (1991).
- <sup>34</sup>R. Kuzuo, M. Terauchi, and M. Tanaka, *Jpn. J. Appl. Phys., Part 1* **31**, 1484 (1992).
- <sup>35</sup>R. F. Egerton and M. J. Whelan, *Philos. Mag.* **309**, 739 (1974).
- <sup>36</sup>R. A. Roberts and W. C. Walker, *Phys. Rev.* **161**, 7730 (1967).
- <sup>37</sup>P. J. Fallon and L. M. Brown, *Diamond Relat. Mater.* **2**, 1004 (1993).
- <sup>38</sup>Y. Iwasa, T. Arima, R. M. Fleming, T. Seigrist, O. Zhou, R. C. Haddon, L. J. Rothberg, K. B. Lyons, H. L. Carter Jr., A. F. Hebard, R. Tycko, G. Dabbagh, J. J. Krajewski, G. A. Thomas, and T. Yagi, *Science* **264**, 1570 (1994).
- <sup>39</sup>L. Marques, J. L. Hodeau, M. Nunez-Regueiro, and M. Perroux, *Phys. Rev. B* **54**, 12633 (1996).